Electronic Supplementary Material (ESI) for Nanoscale.

Electronic Supplementary information

Frequency-dependent learning achieved using semiconducting polymer/electrolyte composite cells

W.S. Dong, [a,b] *F. Zeng,* [a,b]* *S.H. Lu,* [a,b] *A. Liu,* [a] *X.J. Li,* [a,b] *F. Pan*[a]*

[a] Laboratory of Advanced Materials (MOE), School of Materials Science and Engineering, Tsinghua University, Beijing 100084, People's Republic of China

[b] Center for Brain Inspired Computing Research (CBICR), Tsinghua University, Beijing 100084, People's Republic of China

*Corresponding authors

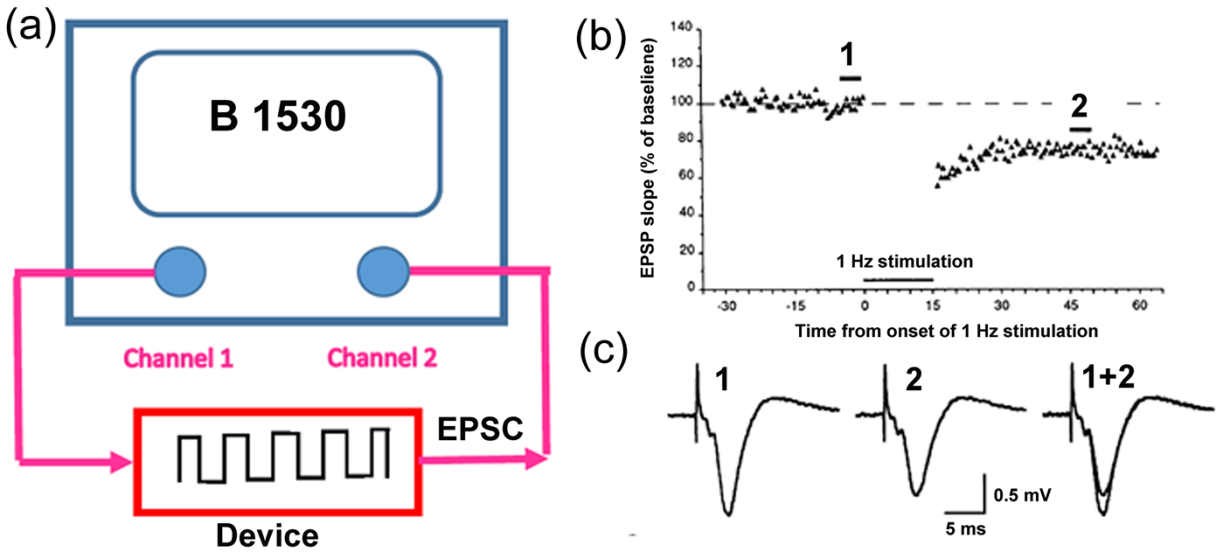

Fig. S1 Schematic of measurement protocol. (a) Testing loop. Agilent B1530 is a waveform generator that could either perform direct current sweeping or generate pulse waveform with modulated shape and frequency. (b) and (c) Calculation of weight modification reported in the paper of Dudek et al.[1]

Fig. S1 illustrates measurement protocol. Agilent B1530 is a signal source that could be used to design pulse shape and series. It owns fast and flexible waveform generation with 10 ns programmable resolution. The minimum pulse width was 100 ns in PG mode or 300 ns in Fast IV mode. It has fast and accurate low current measurement in a resolution of 0.1 nA. The current measurement range is from 1 nA to 10 mA. The minimum current or voltage measurement sampling interval is 5 ns. The two channels could record either current or potential at both ports of our device. The channel connected to the top electrode was used for signal import and the one connected to bottom electrode was used to record EPSC or IPSC. The testing loop was shown in Fig. S1a. The arrows indicate the loading direction. The pulse width in our study was 3~5 ms and the sampling interval was 50 μs. The testing was performed on Cascade 150 platform. The compliant current was set at 1μA and the corresponding bandwidth is 80 kHz.

The measurements of pulse responses in Figs. 1b & c (EPSC or IPSC) corresponded to those

illustrated in Figs. S1b & c reported on Ref. 1, in which the pulse amplitude was 0.5 mV and the pulse width was 5 ms. Label '1' indicates the peak values abstracted from the responses to a set of pulses with baseline frequency of 0.03 Hz. Label '2' indicates those after "1 Hz stimulation" labeled by a horizontal bar. Waveform comparison between '1' and '2', which were plotted together in '1+2'. The weight modification was calculated using the ratio between '1' and '2'. One can see that the value of '2' was smaller than '1'. Thus, the sample displayed long term depression (LTD) after the 1 Hz stimulations.

We also used the discharging peaks in Figs. 1b & c to calculate the weight modification of synaptic plasticity. The frequency selectivity could be demonstrated more clearly in Fig. S6. The red dots of 10 Hz stimulation were evidently lower than those in the responses of the previous baseline frequency, while those of 100 Hz were higher. We performed 1 Hz→1 Hz→1 Hz test before using other higher frequency and did not find weight modification. This indicated that a pulse response relaxed absolutely at 1 Hz frequency. Therefore, we used 1 Hz as baseline frequency for convenience to writing testing program. The frequency lower than 1 Hz or slightly higher than 1 Hz could also be used as baseline frequency, but that did not influence the results in quality.

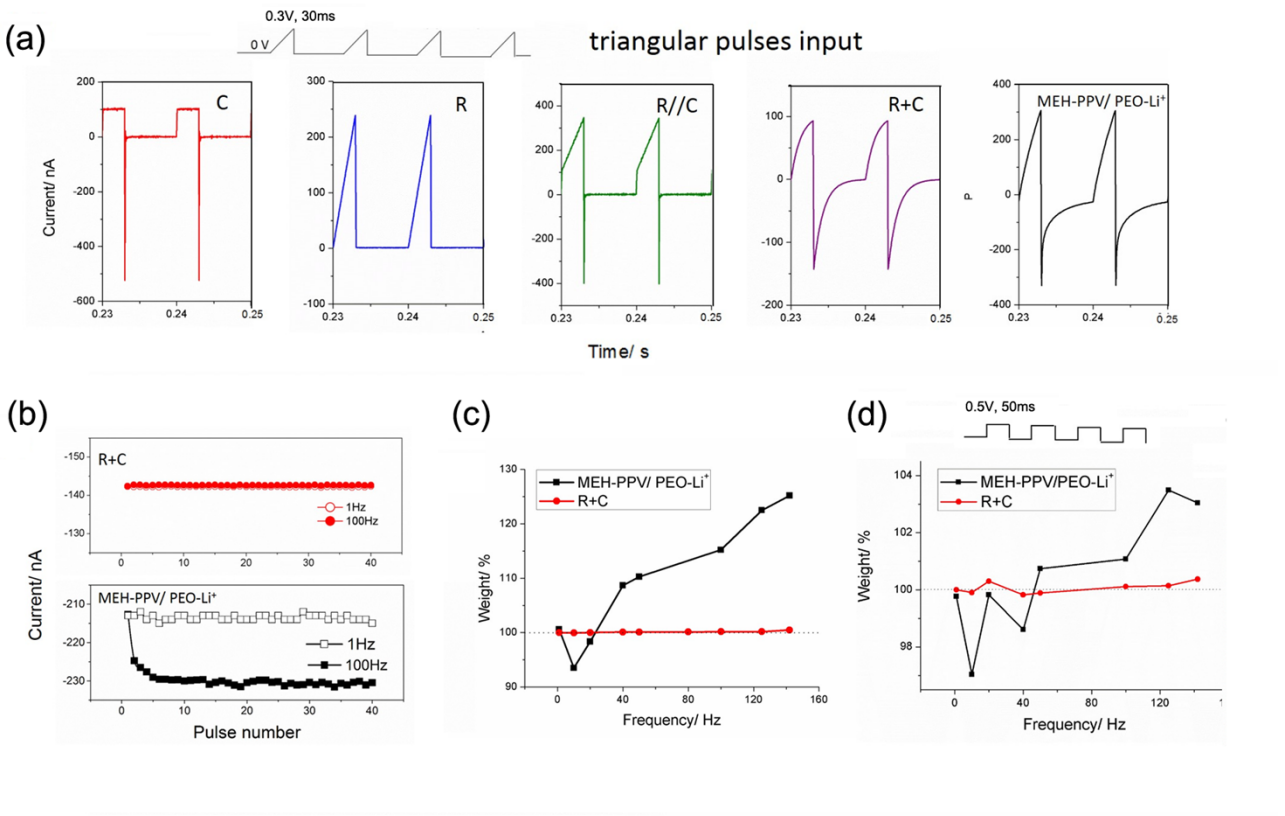

Fig. S2 RC circuitry transient and weight modification measured by 0.3 V triangular pulses ((a) to (c)). (a) Responses to HFS (100 Hz stimulation) of pure capacitor (C=1 nF), pure resistor (R=1.3 MΩ), their connected devices in parallel (R//C) and in series (R+C), and MEH-PPV/PEO-Li^+ cell, separately. (b) Response varied with pulse numbers. Upper part stands for the response of R+C system and lower part stands for the response of MEH-PPV/PEO-Li^+ cell. (c) Weight modification varied with frequencies. (d) Weight modifications obtained by using 0.1 V rectangular pulses. (c) and (d) Black square line stands for weight of MEH-PPV/ PEO-Li^+ cell and red dot line stands for weight of R+C system.

The transient response, i.e. charge and discharge with device impedance, leaky resistance, and parasitic capacitance are critical for high speed and low current measurement and especially using the discharge current. We tested the pulse responses of a pure capacitor (1 nF), a resistor (1.3 MΩ) and their RC circuits connected in parallel (R//C) and in series (R+C), and plotted the results in Fig.

S2. It could be found that under the HFS (i.e. 100 Hz), the resistor (R) followed input signals regularly and no discharging process occurred, suggesting no effective leaky resistance in our measurement system. Meanwhile, the discharging peaks of both C and R//C decayed back into zero or a stable value corresponding to the resistance within only 100 μs (2 sampling points), indicating that the frequency we adopted was actually not high enough to generate parasitic capacitance in measuring circuitry.

Similar overshot charging and discharging current compared with our MEH-PPV/PEO-Li^+ cell could be found in the R+C system. However in R+C system, the value of discharging peaks (I_A) were fixed with pulse numbers, regardless of the frequency values, which was significantly different from that in the MEH-PPV/PEO-Li^+ cell (Fig. S2b). Furthermore, the weight modification *vs* frequency was also presented in Fig. S2c and no obvious weight variation was found in R+C system. Besides, the MEH-PPV/PEO-Li^+ cell displaysed similar frequency selectivity by changing the pulse mode to 0.1 V rectangular pulses (Fig. S2d), while the R+C circuit did not show frequency selectivity yet. So it could be illustrated that dynamic equilibrium of stimulations or RC delay of the measuring circuitry could not account for the responses of our cells, including frequency selectivity.

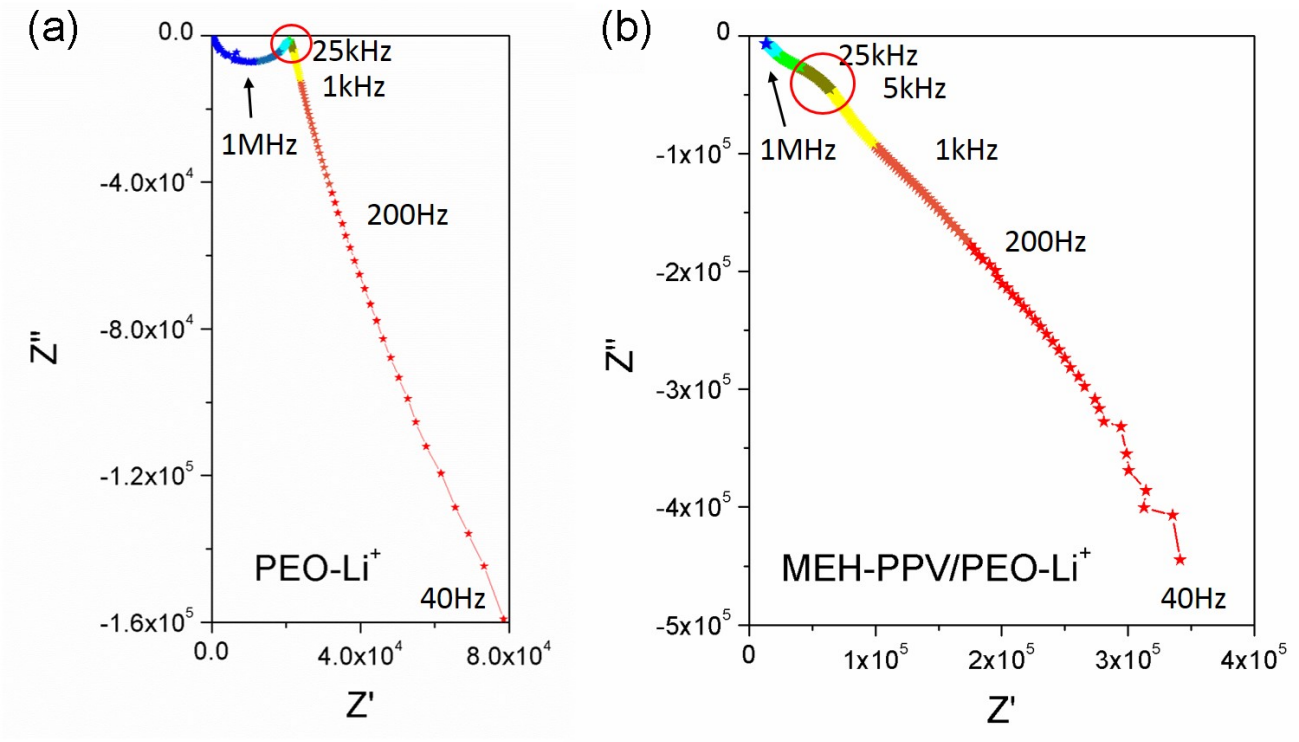

Fig. S3 Nyquist impedance of (a) PEO-Li^+ (b) MEH-PPV/PEO-Li^+ from 40 Hz to 1 MHz.

Nyquist impedance of PEO-Li^+ for frequency range from 40 Hz to 1 MHz was then shown in Fig. S3a, representing a typical ion-conducting system for a single semicircle at high frequencies and a capacitive tail at low frequencies. We used the method reported in Ref. 2 to give an equivalent circuit for the standard analysis and then obtained σ of 1.18×10^{-3} S/cm in our PEO+Li^+ device.[2] The capacitive tail of PEO-Li^+ at low frequencies, which was also presented in Fig. S3b of MEH-PPV/PEO-Li^+ double layer, indicating the presence of ionic transportation. The slope of capacitive curve in Fig. S3a was much bigger than that in Fig. S3b, representing a much faster ion transport velocity of pure PEO-Li^+ than MEH-PPV/PEO-Li^+ layers, which should be resulted from the significantly modulated ion migration at the polymer/electrolyte interface. After covered on MEH-PPV layers, the semicircle part of PEO-Li^+ disappeared but left an inflection point of impedance curve still at around 25 kHz. Since parasitic capacitance is actually a high frequency phenomena, in the measuring rage which we used for frequency dependence plasticity (f<200Hz), MEH-PPV/ PEO-Li^+ double layer cells would

behave only capacitive, the impedance of which was almost a straight line so that the effect of parasitic capacitance could be I ignored.

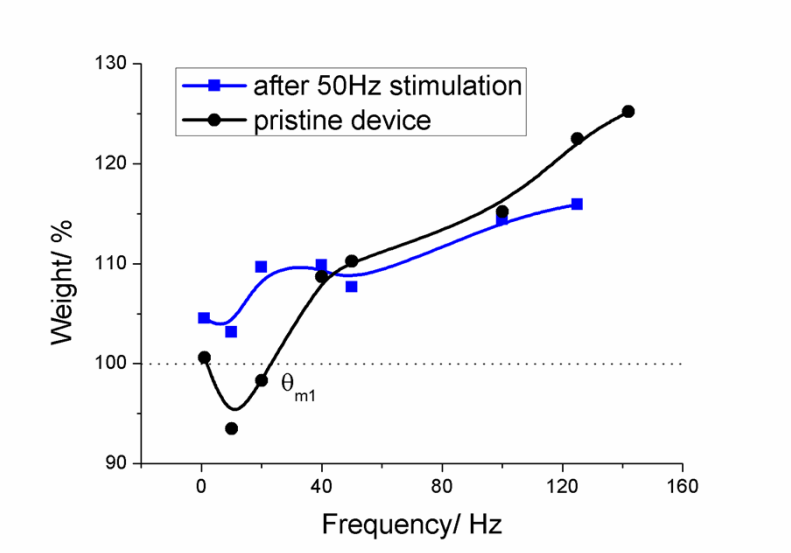

Fig. S4 Weight modifications of various stimulations fowllowing a 50 Hz stimulation.

An experiment was performed in which a train of high frequency pulses (i.e. 50Hz) first were loaded and followed by the stimulations with other frequencies. A potentiation at all frequencies was only observed and a left threshold shift was not obtained (Fig. S4).

The LTP/LTM of a specific stimulation was measured on an individual device with the measurement protocol: 1 Hz (baseline) →10 Hz (stimulation)→ 1 Hz (read)→ 1 Hz (read)→ 1 Hz (read). One device corresponded to one stimulation except the measurements of Fig. 2b and Fig. S4. Therefore, the SRDP and LTP/LTM was not claimed to be achieved simultaneously on one device.

Usually, we prepared several pieces of samples in a round of experiment. This could avoid exposing the samples in air for long time. At the same time, we had considered the question about the device-device influence, i.e., whether the modified device influenced the others. Up to now, we did not find that the weight modifications were affected by the neighboring device on the same piece. For instance, we specifically selected several typical devices coming from different substrates

and listed the testing results in Table S1. Their resistances (or impedances) varied in a relative large range, which should be related to the drop-cast technique. The thickness and roughness varied greatly. As shown in Table S1, device 1 on piece A and device 2 on piece B responded in depression to 10 Hz inputs regardless of different substrate. Device 3 on piece A and device 4 on piece C responded in potentiation to 100 Hz inputs regardless of different substrate. Device 3 on piece A was not affected by the tested neighboring device 1, and the value of discharging peak was even lower than that of device 1 on piece A. The results in Table S1 also give indirect supports for two issues. First, the frequency selectivity occurred due to the effects at the polymer/electrolyte interface. Second, the structural images of Figs. 4b & c suggested ionic channels in PEO were conducted perpendicular to the MEH-PPV layer (Fig. 5b).

Table S1. The measurement results from the samples of three substrates

		Discharging peak (nA)			Calculated weight (%)		
Piece	Device	1 Hz	10 Hz	1 Hz	1 Hz	10 Hz	1 Hz
A	1	−131	−123	−127	100	93.29	96.68
B	2	−254	−223	−224	100	87.81	88.20
		1 Hz	100 Hz	1 Hz	1 Hz	100 Hz	1 Hz
A	3	−66.9	−77.8	−78.6	100	116.29	117.49
C	4	−233	−267	−258	100	114.59	110.73

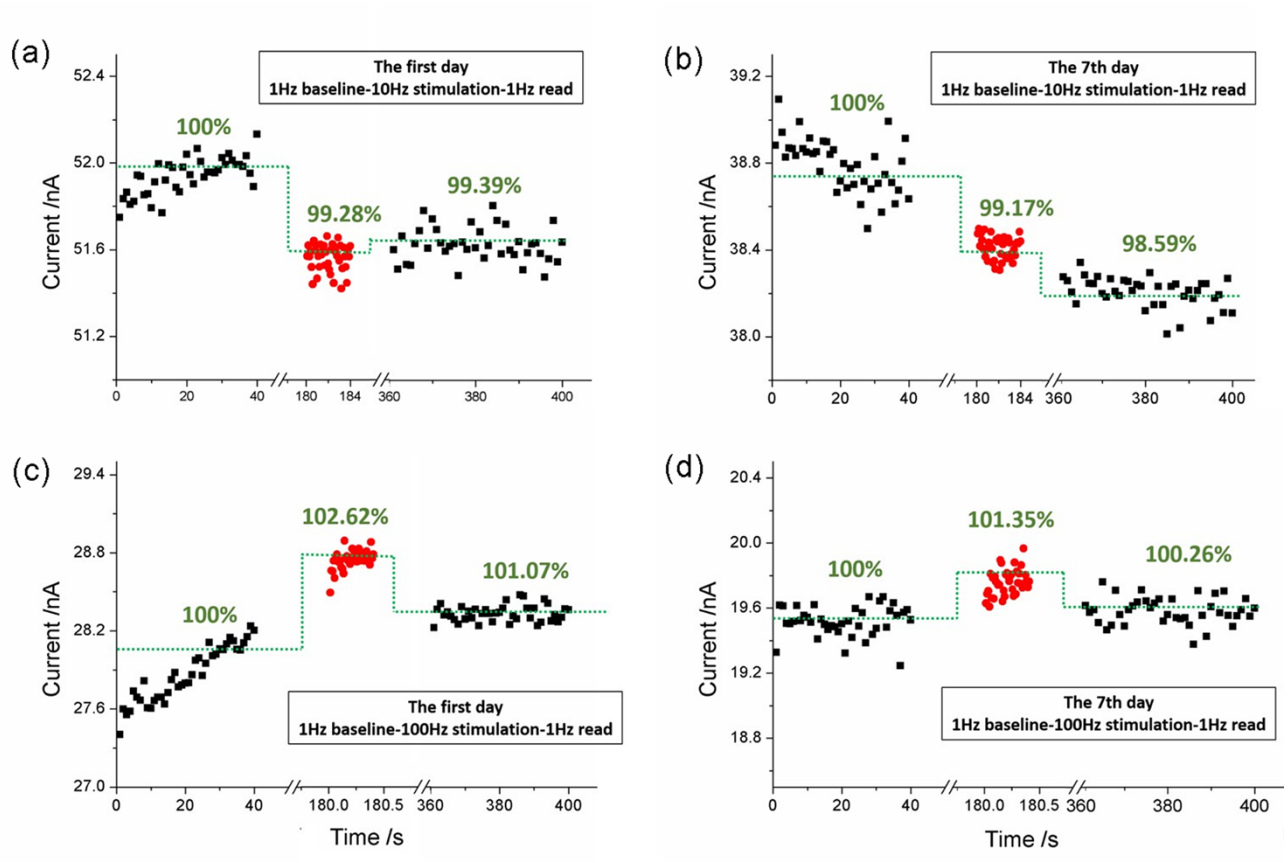

Fig. S5. Retention of the cells. (a) The cell responded to depression at 10 Hz stimulations. It displayed the same behavior (b) in the 7th day. (c) The cell responded to potentiation at 100 Hz stimulations. It displayed the same behavior (d) in the 7th day. The pulse amplitude was 0.1 V and the pulse duration was 50 ms.

The retention of the cells was examined by testing the cell twice in a week. Fig. S5 shows the results using two typical frequencies corresponding to depression at 10 Hz stimulations and potentiation at 100 Hz stimulations shown in Fig. 1. Fig. S5a shows that the cell responded to depression at 10 Hz stimulations and Fig. S5c shows that the cell responded to potentiation at 100 Hz stimulations. One can see that they displayed the same behavior in the 7th day. This indicated that the cell could conserve their properties longer than a week. The peak values in Fig. S5 were slightly lower than those in Fig. 1b. That might be due to or inhomogeneous thickness or salt distribution in PEO. The peak values in Fig. S5 decreased in an extent in the 7th day. This might be

due to the aging effect after exposure in air. We estimated the rate of this current decay according to the data in Fig. S5, which would be 0.02% in the measurement period of about 400s. Thus, it can be concluded that the properties of frequency selectivity could be extended to several days. We did not find that this uncertain decay mechanism played dominate role during in the measurement period. Sealing the device or performing measurements under certain atmosphere or solvent might exclude the unknown decay effect. This issue is very significant and need deliberate experimental design in the future. Moreover, an individual synapse usually could not endure test again and again. Since the activated zones of our device and biological synapse are organic materials, there might exist common unknown decay mechanism.

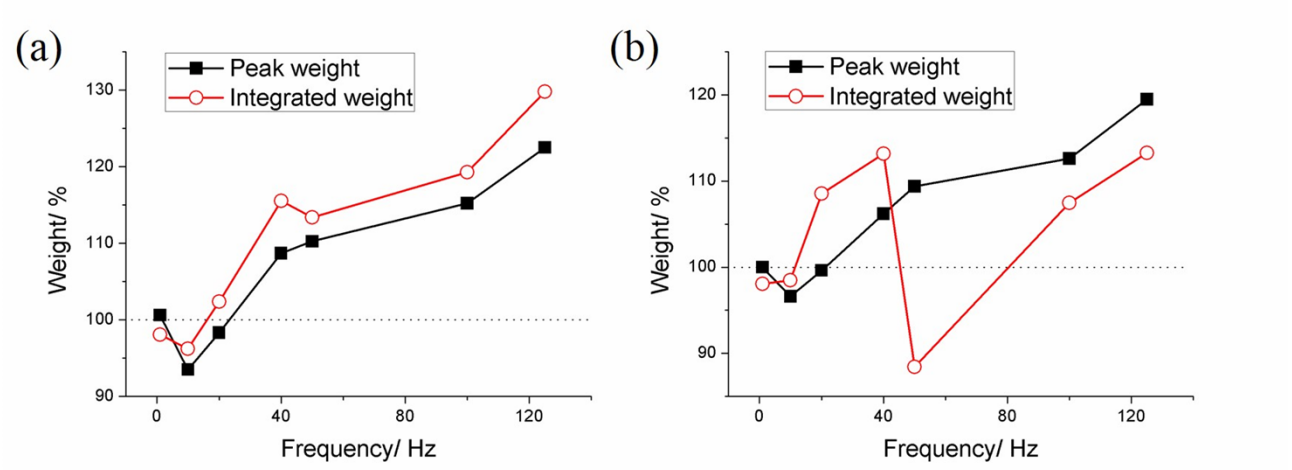

Fig. S6 Integrated Weights calculated according to the responses to (a) stimulation and (b) 1 Hz read pulses with triangular pulse and 0.3 V amplitude.

Many studies in neuroscience have reported to calculate weight modification by integrating the EPSC. Usually, the integrated weight is consistent with the weight calculated from the discharging peak, especially for short term plasticity.[3] We also calculated the weight by integrating the discharging progress of the last pulse response as shown in Fig. S6. One can clearly see that the integrated weights varied in the same trend with the peak weights for the stimulation processes (Fig. S6 a). However, when we handled the data of 1 Hz read after the stimulation, the integrated

weight differed from the peak weight in many frequencies (Fig. S6 b). The integrated weight might influenced greatly by many factors, such as the integration limit, environment noise and background of matrix. For the resting state (i.e., 1 Hz frequency), the peak strength might reflect the system state appropriately in the view of saving energy.

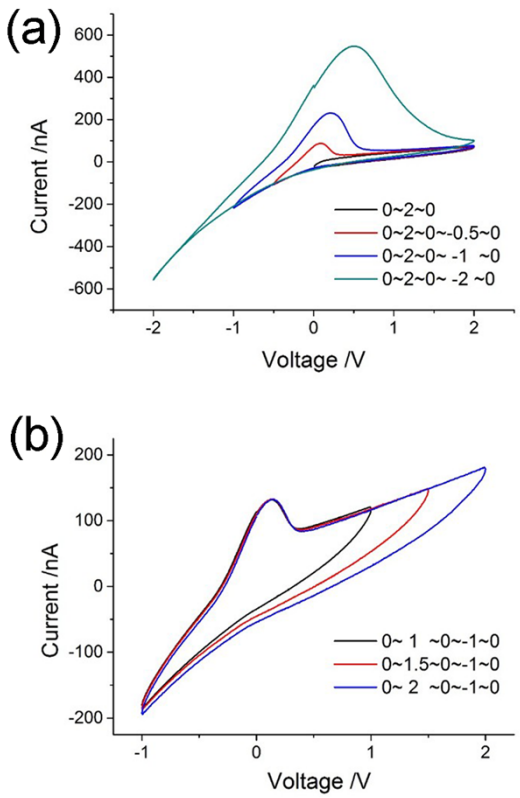

Fig. S7. Direct current-voltage (I-V) properties obtained from various sweep cycles. (a) The negative parts in the sweep cycle varied from -0.5 to -2 V, while the positive parts were fixed at 2 V. (b) Positive parts in the sweep cycle varied from 1 to 2 V, while negative parts were fixed at -2 V.

Two sweep cycles were performed to test ion kinetics at the interface and in the PEO matrix. First, the positive part of the sweep cycle was fixed at approximately 2 V, but the negative part varied from 0 to -2 V. One can see that the current value induced by the initial positive bias was very low but increased quickly after the bias was turned negatively. If the bias was swept back from the negative to the positive, NDR appeared in the range of positive bias. The larger the negative

bias was added, the stronger the NDR effect (Fig. S7a). Second, the negative part in the sweep cycle was fixed at approximately -1 V, but the positive part varied from 0 to 2 V. The NDR appeared stably in each case near 0.1 V, when the bias changed from a negative quadrant to a small positive quadrant (Fig. S7b). These two results suggested that NDR was dependent on the ions driven back to the electrolyte matrix by the negative bias. These ions were confined in fibrous nano-channels in a PEO matrix after the negative sweep. They were not able to diffuse smoothly at the interface due to the rapid following positive bias so that an instantaneous opposite electrical field was formed to result in NDR.

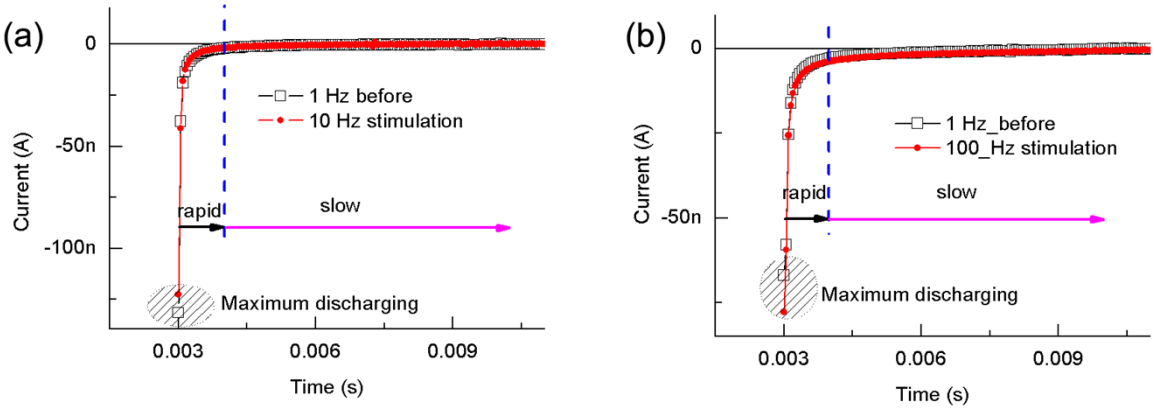

Fig. S8 Comparison of discharging shapes obtained by using a train of pulses with amplitude of 0.3 V and pulse width of 3 ms. (a) 1 Hz→10 Hz; (b) 1 Hz→100 Hz.

Fig. S8 compared the discharging shapes abstracted from the pulse responses of various trains of 0.3 V triangular pulses. Apparently, they were quite different from the typical capacitor, resistor and R+C circuit. The total discharging process cannot be fitted by using a simple exponent decay curve. The discharging process mainly composed of a rapid range and a slow range. The current in the former was high and decayed quickly, while that in the later was low and decayed slowly. The rapid range was estimated around 1 ms. The current during the slow range could be influenced by the environment noise due to the limitation of instruments resolution, so that its effective time

constant is hard to be estimated. The total relaxation time of a discharging process should be actually long enough for either LFS or HFS. We thought that the system state was determined by the rapid range and fitted the data in 1 ms by using a simple exponent decay function. The fitting results were well consistent with the experimental and were listed in Table 1. Similar discharging process can be found in the responses of memristor with faster decay initially, [4] of which the time constant was also quiet larger than that of electron in a pure capacitive system as well as that in our cells. Considering oxygen vacancy was the principal resistive switching mechanism,[4] we thought that ionic migration or interfacial de-polarization account for the rapid range of the discharging process in both our cell and memristor.[5]

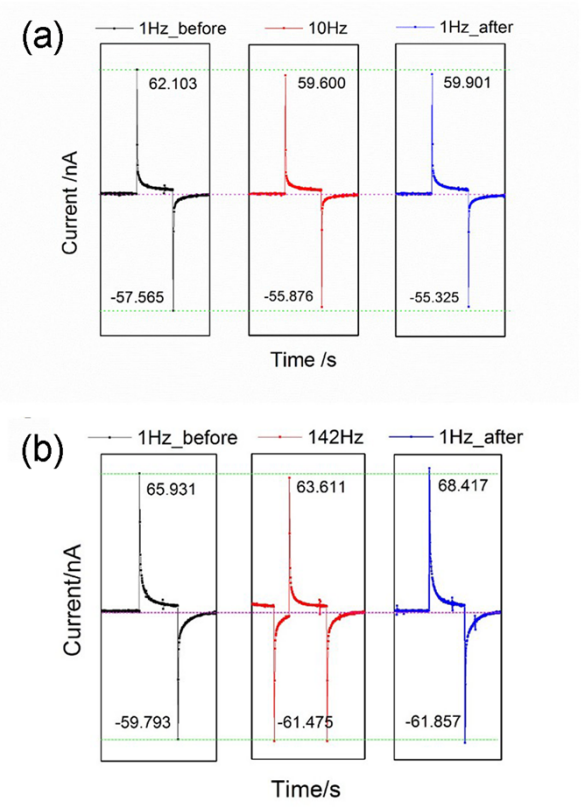

Fig. S9. Comparison among the last responses obtained from two different measurement schedules. (a) A train of 1 Hz pulses→ 10 Hz stimulations→ 1 Hz pulses. (b) A train of 1 Hz pulses → 142 Hz stimulations → 1 Hz pulses.

Long term plasticity after low frequency stimulations (LFS, ~10 Hz)) could be observed in Fig. S8a. The LFS reduced both doping (charging) and de-doping (discharging) current during the stimulation process and the following 1 Hz read pulses took the same behaviour. However, high frequency stimulation (HFS, ~142 Hz) enhanced the de-doping current but not the doping current during stimulation, while both of the doping and de-doping current of 1 Hz read pulses were increased after HFS (Fig. S8b). This suggested that HFS increased the activated channels in the PEO electrolyte.

References:

1. Dudek, S. M.; Bear, M. F., Homosynaptic Long-Term Depression in Area Ca1 of Hippocampus and Effects of N-Methyl-D-Aspartate Receptor Blockade. *PNAS* **1992**, *89*, 4363-4367.
2. Patel, S. N.; Javier, A. E.; Stone, G. M.; Mullin, S. A.; Balsara, N. P., Simultaneous Conduction of Electronic Charge and Lithium Ions in Block Copolymers. *ACS Nano* **2012**, *6*, 1589–1600.
3. David L. Brody and David T. Yue, Release-Independent Short-Term Synaptic Depression in Cultured Hippocampal Neurons,. *J. Neurosci.* **2000**, *20*, 2480-2494.
4. Kim, S.; Du, C.; Sheridan, P.; Ma, W.; Choi, S. H.; Lu, D. W., Experimental Demonstration of a Second-Order Memristor and Its Ability to Biorealistically Implement Synaptic Plasticity. *Nano Lett.* **2015**, *15*, 2203-2211.
5. Tang, G. S.; Zeng, F.; Chen, C.; Liu, H. Y.; Gao, S.; Song, C.; Lin, Y. S.; Chen, G.; Pan, F., Programmable Complementary Resistive Switching Behaviours of a Plasma-Oxidised Titanium Oxide Nanolayer. *Nanoscale* **2013**, *5*, 422-428.